

Theoretical Study for Autoionization of Liquid Water: Temperature Dependence of the Ionic Product (pK_w)

Hirofumi Sato and Fumio Hirata*

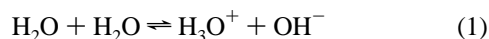
Division of Theoretical Study, Institute for Molecular Science, Okazaki, 444, Japan

Received: October 16, 1997

The temperature dependence of the ionic product of water (pK_w) is investigated theoretically by means of ab initio electronic structure theory combined with the extended reference interaction site method in statistical mechanics of molecular liquids (RISM-SCF/MCSCF method). The chemical equilibrium $H_2O + H_2O \rightleftharpoons H_3O^+ + OH^-$ is studied, in which water molecules, hydronium ions, and hydroxide ions are regarded as “solute” molecules in aqueous solution. Molecular geometries, electronic structures, pair correlation functions, and free energy components of those species as well as their temperature dependence are calculated. It is shown that the hydroxide anion is polarized more easily by surrounding solvent compared to the other species. The solvent-induced electronic structure relaxes toward that in the gas phase as temperature increases. The hydroxide anion exhibits the largest temperature dependence in the electronic structure as well as in solvation structure. It is found that changes in the solvation free energies drive the chemical equilibrium toward the left-hand side (association) as temperature increases, while energies associated with solvent-induced reorganization of electronic structure make the opposite contribution. The temperature dependence of pK_w is dominated by the latter contribution, which gives rise to good agreement with the experimental results. It is suggested that the observed temperature dependence of pK_w is related to the great sensitivity of the electronic structure of OH^- on the solvent effect.

1. Introduction

A water molecule has *amphoteric* character, which means it can act as both an acid and a base. The autoionization equilibrium process in water,



is one of the most important and fundamental reactions in a variety of fields in chemistry. The ionic product defined by

$$K_w = [H_3O^+][OH^-] \quad (2)$$

and its logarithm

$$pK_w = -\log K_w \quad (3)$$

are measures of the autoionization. The quantity can be related to the free energy change (ΔG) associated with the reaction of eq 1 by the standard thermodynamic relation¹

$$\Delta G = 2.303RTpK_w \quad (4)$$

The free energy change consists of various contributions including changes in the electronic energy and “solvation” free energy of the molecular species concerning the reaction, which are related to each other. A microscopic description of the reaction, therefore, requires a theory that accounts for both the electronic and liquid structures of water.

Many theoretical attempts have been made to evaluate pK_w and pK_a values in aqueous solutions, which involve determination of molecular parameters for H_3O^+ and OH^- ions in the liquid.^{2–7} Most of them have employed the molecular simulation techniques combined with the standard ab initio molecular

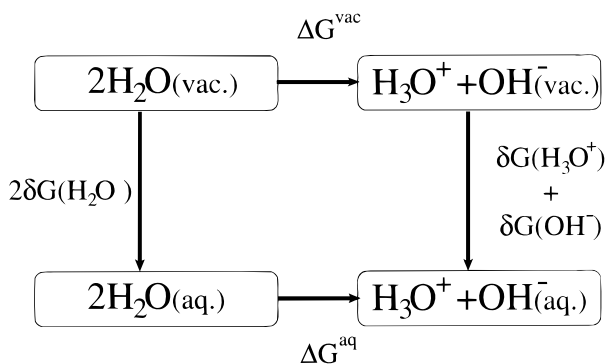
orbital method. However, the prediction of pK_w is usually very difficult since it requires high accuracy in the description of the electronic and liquid structures as well as their coupling. The RISM-SCF/MCSCF method, developed recently,^{8,9} has been successfully applied to a variety of chemical processes in solution phase.^{8–10} The method is ab initio electronic structure theory combined with the extended reference interaction site method,^{11,12} in statistical mechanics of a molecular liquid. The RISM-MCSCF method calculates simultaneously electronic structure and molecular geometry of a solute molecule as well as statistical solvent structure in a self-consistent manner.⁹ The method, therefore, is expected to provide a powerful tool to tackle the problem of primary importance in chemistry.

It is experimentally known that the pK_w value shows significant temperature dependence; i.e., it decreases with increasing temperature.¹³ The observation apparently contradicts an intuitive consideration with respect to the effect of hydrogen bonding on intramolecular O–H bond and its temperature dependence. Rising temperature must intensify the rotational and translational motion of each water molecule, and the hydrogen bondings are weakened. If the above autoionization process is only governed by the hydrogen bond strength alone, it is feasible that the equilibrium leans toward the left-hand side of the equation.

In the present report, we apply this method to investigate the temperature dependence of pK_w . We also discuss geometrical structures and hydration structure of related species, as well as their temperature dependence.

2. Computational Details

To facilitate the calculation of the free energy change ΔG^{aq} associated with the reaction in eq 1, we use a thermodynamic

SCHEME 1: Thermodynamic Cycle of Autoionization of Water

cycle illustrated in Scheme 1, regarding the species concerning the reaction as a “solute” in infinitely dilute aqueous solution. (We use “ Δ ” for changes of quantities associated with the chemical reaction and “ δ ” for changes due to solvation. Superscripts “aq” and “vac” are used to distinguish aqueous and vacuum environments.) Then, ΔG^{aq} can be written in terms of the energy change associated with the reaction in vacuo ΔG^{vac} and the free energy change of the reacting species due to solvation as

$$\Delta G^{\text{aq}} = \Delta G^{\text{vac}} + \delta G(\text{H}_3\text{O}^+) + \delta G(\text{OH}^-) - 2\delta G(\text{H}_2\text{O}) \quad (5)$$

where $\delta G(\text{H}_3\text{O}^+)$, $\delta G(\text{OH}^-)$, and $\delta G(\text{H}_2\text{O})$ are respectively the free energy changes of H_3O^+ , OH^- , and H_2O upon solvation. The free energy change δG for each species can be decoupled into intra- and intermolecular contributions as

$$\delta G = \delta G^{\text{intra}} + \delta \mu \quad (6)$$

where δG^{intra} is the intramolecular contribution consisting of the changes in the kinetic (translational, rotational and vibrational) terms and the electronic reorganization energy,

$$\delta G^{\text{intra}} = \delta G_{\text{kin}} + \delta E_{\text{elec}} \quad (7)$$

The electronic reorganization energy is defined as difference of the electronic energies between

$$\delta E_{\text{elec}} = E_{\text{elec}}^{\text{aq}} - E_{\text{elec}}^{\text{vac}} \quad (8)$$

where $E_{\text{elec}}^{\text{aq}}$ and $E_{\text{elec}}^{\text{vac}}$ are the electronic energy in solution and in vacuo, respectively.^{10b} The intermolecular contribution, $\delta \mu$, is the excess chemical potential or the solvation free energy. From eqs 5–8, we have

$$\Delta G^{\text{aq}} = \Delta E_{\text{elec}}^{\text{vac}} + \Delta \delta G_{\text{kin}} + \Delta \delta E_{\text{elec}} + \Delta \delta \mu \quad (9)$$

where

$$\Delta E_{\text{elec}}^{\text{vac}} = E_{\text{elec}}^{\text{vac}}(\text{H}_3\text{O}^+) + E_{\text{elec}}^{\text{vac}}(\text{OH}^-) - 2E_{\text{elec}}^{\text{vac}}(\text{H}_2\text{O})$$

$$\Delta \delta G_{\text{kin}} = \delta G_{\text{kin}}(\text{H}_3\text{O}^+) + \delta G_{\text{kin}}(\text{OH}^-) - 2\delta G_{\text{kin}}(\text{H}_2\text{O})$$

$$\Delta \delta E_{\text{elec}} = \delta E_{\text{elec}}(\text{H}_3\text{O}^+) + \delta E_{\text{elec}}(\text{OH}^-) - 2\delta E_{\text{elec}}(\text{H}_2\text{O})$$

$$\Delta \delta \mu = \delta \mu(\text{H}_3\text{O}^+) + \delta \mu(\text{OH}^-) - 2\delta \mu(\text{H}_2\text{O})$$

In the above equations, $\Delta E_{\text{elec}}^{\text{vac}}$ which concerns the electronic structures of the species only in the gas phase, can be calculated from the standard ab initio MO method. $\Delta \delta E_{\text{elec}}$ and $\Delta \delta \mu$ are

our major concerns in the present study, which requires a self-consistent determination of the electronic structure and the statistical solvent distribution. We employ the RISM-SCF procedure to calculate those quantities.⁹ $\Delta \delta G_{\text{kin}}$ can be obtained from the elementary statistical mechanics given the optimized molecular geometry for the reacting species in gas and solution phases. Optimizing molecular geometry in the solution phase, however, is not a standard problem, which requires calculation for energy gradients of a solvated molecule. The RISM-MCSCF method, which has been proposed recently, enables us the geometry optimization of a molecule in solution phases.

Since details of the RISM-SCF/MCSCF method are reported elsewhere,⁸ here we make brief comments concerning approximations and models used in the present study. For the electronic structure calculations, the standard triple- ζ basis set augmented by p polarization functions on hydrogen atoms and d polarization function and diffusive p function ($\alpha_p = 0.059^{14}$) on oxygen atom is employed in the Hartree–Fock (HF) method. Molecular geometries of all the species (H_2O , H_3O^+ , and OH^-) are optimized in both gas and solution phases under a constraint that H_2O and H_3O^+ are assumed to possess C_{2v} and C_{3v} symmetry, respectively.

In solving the RISM equation, we employ a SPC-like water model¹⁵ which has been successful in liquid-phase calculations. The same Lennard-Jones parameters are used for H_3O^+ and OH^- . The experimental density of water and its temperature dependence, which are taken from the literature,¹⁶ are used in the calculation.

Our primary concern in the present study is the temperature dependence of $\text{p}K_w$ in the aqueous phase. So, we concentrate our attention on the relative value of $\text{p}K_w$ at temperature T to that at $T = 273.15$ K chosen as a standard, that is,

$$\begin{aligned} \Delta_{\text{T}} \text{p}K_w(T) &= \text{p}K_w(T) - \text{p}K_w(273.15) \\ &= \frac{1}{2.303R} \left\{ \frac{\Delta G^{\text{aq}}(T)}{T} - \frac{\Delta G^{\text{aq}}(273.15)}{273.15} \right\} \quad (10) \end{aligned}$$

The difference of the electronic energies in vacuo, $\Delta E_{\text{elec}}^{\text{vac}}$, makes a dominant contribution to determine the “absolute” value of $\text{p}K_w$. However, $\Delta E_{\text{elec}}^{\text{vac}}$ is essentially independent of T , and it contributes to temperature dependence of $\text{p}K_w$ in the aqueous phase only through $1/T$ in eq 10.

3. Results and Discussion

3.1. Solvent Effect on Molecular Geometry and Its Temperature Dependence. Our computational results for the molecular structure of liquid water are shown in Table 1 along with other experimental and theoretical results reported previously. The experimental values for HOH angles are obtained from corresponding data for average OD and DD distances, $\langle r(\text{OD}) \rangle$ and $\langle r(\text{DD}) \rangle$. Our result predicts elongation of the OH bond by 0.015 Å upon transferring H_2O from gas to liquid, which is in qualitative accord with all previous results obtained from both theoretical calculations and experiments. The results are in harmony with the intuitive argument that hydrogen atoms of a water molecule in liquid phase are “pulled” by oxygen atoms in other molecules due to hydrogen bonding. In a more general class of liquids such as a system of hard spheres, an apparent attractive force acts between two neighboring particles due to thermal pressure effects from surrounding molecules.¹⁷ Such a force may cause shortening of chemical bonds of molecules in the liquid phase.^{18,19} However, in water, the effect will not show up, because hydrogen atoms are deeply embedded

TABLE 1: OH Bond Lengths and HOH Angles for Liquid Water and Their Changes As Moving from the Gas to the Liquid Phase^a

	OH		HOH		ref	
	length	change	angle	change		
Experimental						
Thiessen et al.	0.996	+0.009	102.8	-1.7	24	298 K mixture of the isotopic species
Walford et al.	0.98	+0.023	105.5	+1.0	25	294 K, D ₂ O
Ichikawa et al.	0.970	+0.013	106.6	+2.1	21	298 K, D ₂ O
Theoretical						
present work	0.956	+0.015	106.1	-1.0		293 K
Corongiu et al.	0.978	+0.021	101.1	-3.4	22	305 K, MD
Chipot et al.	0.965	+0.003	105.0	-0.4	3	SCRFF
Moriarty et al.	0.951	+0.010	110.2	+4.1	26	QMSTAT
Chesnut et al.	0.987	+0.017	98.5	-5.2	27	300 K, MD

^a Values are given in angstroms and degrees. Changes in experimental studies are calculated from the gas-phase standard geometry of water, $r(\text{OH}) = 0.9572 \text{ \AA}$ and $\theta(\text{HOH}) = 104.52^\circ$, while theoretical predicted changes are from individual isolated water model.

in the oxygen core, so that the thermal pressure will not acts on the pair of O and H atoms in a molecule. The results concerning the HOH angles show a large diversity in both experimental and theoretical works even in their sign. Two effects of solvation on the bond angles, which counteract each other, are conceivable. The solvation causes increase in the effective charges on atoms or polarizes a molecule, which will make the HOH angle wider due to the increased electrostatic repulsion between hydrogen atoms in a molecule.²⁰ On the other hand, narrowing of the angle seems favored from the standpoint of increased dipole moment, since increase in dipole moment gives rise to greater stabilization due to the intermolecular interaction. The HOH angle in liquid water seems to be determined by the subtle balance between those counteracting effects. A theoretical calculation with much higher accuracy will be required to determine whether the HOH angle widens or narrows in liquid water. Our result, which shows narrowing of the HOH angle upon solvation, indicates the latter effect is slightly dominant. There is another conceivable effect due to the thermal pressure effect which likely causes narrowing of the HOH angle. However, the possibility can be ruled out because the hydrogen atoms are well inside the oxygen core.

The calculated temperature dependencies of optimized structure, bond length $r(\text{OH})$ and $\theta(\text{HOH})$, in water are plotted in Figure 1 in the range between 273.15 and 373.15 K. As the temperature increases, $r(\text{OH})$ monotonically shortens. Although the change in bond length is very small, less than 0.006 \AA in this range, the direction of change is opposite to that expected from a naive consideration of the unharmonicity in the potential function for the O–H bond. The shortening in the bond length with rising temperature can be explained in terms of reduced hydrogen bonding due to increased thermal motions, if the elongation of the O–H bond in the liquid is caused by the hydrogen bond. The angle of HOH also shows a small dependence and widens along the upturn of temperature. A neutron diffraction investigation of heavy water by Ichikawa et al.²¹ concluded the values $r(\text{OD})$ and $r(\text{DD})$ remain unchanged in the range between 25 and 200 °C within experimental errors. On the other hand, Corongiu et al. reported the appreciable temperature dependence²² in their study for heavy and light water by molecular dynamics simulations as well as X-ray and neutron scattering. Our results show a decrease in the bond length and widening in the bond angle with increasing temperature, being in accord with the report by Corongiu et al. A reasonable interpretation can be given to the behavior if the HOH angle in fact narrows upon transferring the molecule from gas to liquid phases due to the reasons stated above.

$r(\text{OH})$ and $\theta(\text{HOH})$ in H_3O^+ and OH^- molecules in aqueous

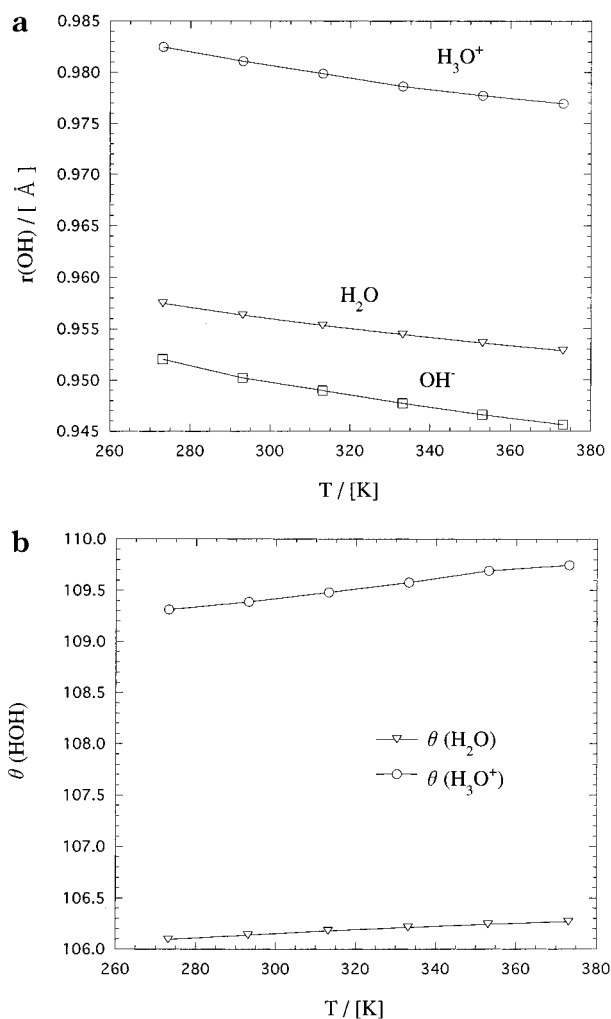


Figure 1. Temperature dependence of water, hydronium ion, and hydroxide ion geometry: (a) bond length of O–H; (b) bond angle of H–O–H.

solutions show a similar tendency in temperature dependence with that we found for a water molecule (Figure 1). Computed geometrical changes are slightly enhanced in these ionic species than in neutral water molecule, presumably due to a stronger hydration by surrounding solvent.

Unfortunately, we could not find any reports about the temperature dependence of these geometric parameters in both experimental and theoretical studies. Geometrical change of H_3O^+ upon moving from gas to the solution phase is reported by Chipot et al.³ Although they optimized the geometry in a

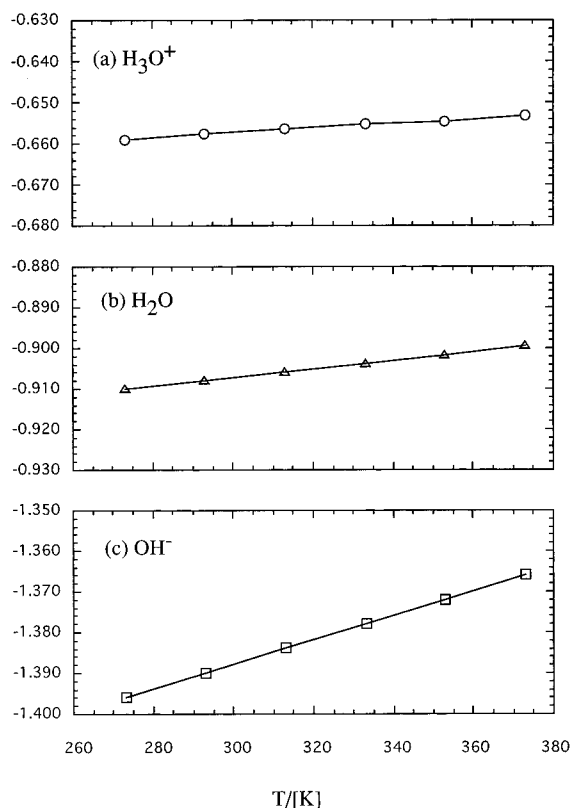


Figure 2. Temperature dependence of electronic structure represented by effective charge on oxygen site: (a) hydronium ion; (b) water; (c) hydroxide ion.

dielectric continuum media mimicking liquid water, qualitative agreement is found in lengthening of $r(\text{OH})$ and narrowing of $\theta(\text{HOH})$ compared with equilibrium geometry of an isolated molecule.

3.2. Solvent-Induced Molecular Polarization and Solvation Structure. Temperature dependence of effective charges on oxygen atoms q_O , which represents a change in the electronic structure induced by solvent effect, is shown in Figure 2. The effective charges were determined in such a way that electrostatic potential produced by the charges fits best with those arising from the electronic cloud of the solute.⁸ Compared with the gas-phase values, -0.766 (water), -0.633 (hydronium ion), and -1.128 (hydroxide ion), charges in all the species are largely enhanced by the interaction with surrounding solvent molecules. The change in the electronic structure or the polarization is appreciably reduced as temperature increases. The behavior can be explained in terms of the increased molecular motion such as rotation. As the motions increase, the hydrogen bond between the solute species and solvent molecules is weakened, and the polarizing effects becomes less and less. Consequently, the electronic structure is relaxed toward that in the isolated molecule as temperature increases. Among three species, the greatest relaxation of polarization is observed in the hydroxide ion, which can be understood in terms of the temperature dependence of the hydration structure of "solute" molecules.

In Figure 3, we show three sets of pair correlation functions (PCF) between (a) solute oxygen and solvent hydrogen and (b) solute hydrogen and solvent oxygen, at 293.15 K. It is readily seen that sharp peaks are found around 2.0 Å in a pair of the ionic species and atoms with opposite charges in water molecules. An oxygen atom in the hydroxide ion has a large negative charge and attracts hydrogen sites of solvent water acutely. In contrast, a hydrogen atom in the hydronium ion

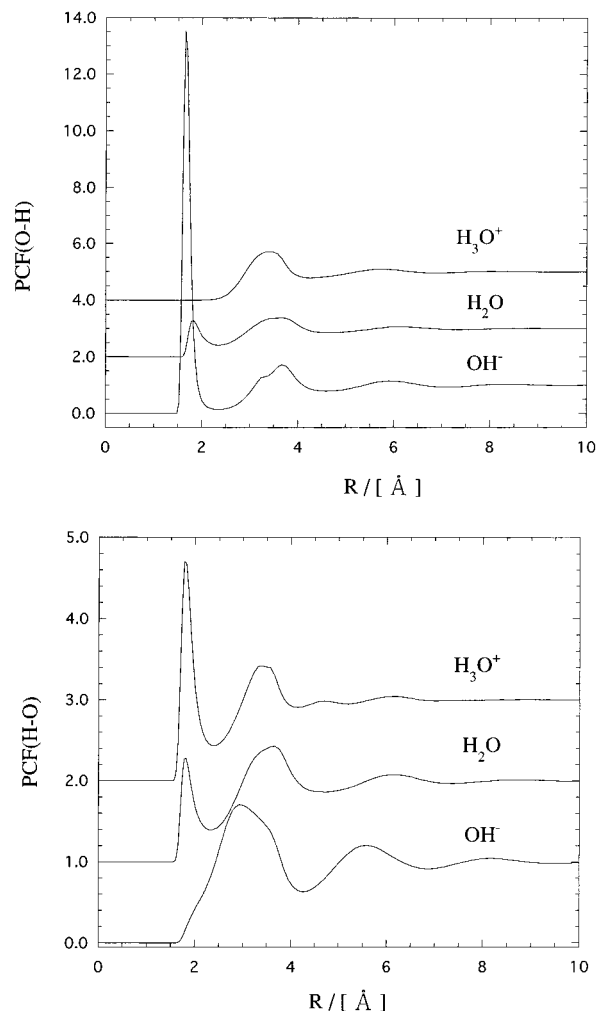


Figure 3. Pair correlation function (PCF) at room temperature (293.15 K): (a) solute oxygen and solvent hydrogen; (b) solute hydrogen and solvent oxygen.

attracts oxygen sites of solvent, but in a moderate manner. Water has an intermediate character of these two ions. The highest peak in PCF between hydroxide O and water H concerns the greatest effective charge of this ion shown in Figure 2. The results indicate that the electronic structure of the hydroxide ion is most sensitive to the electrostatic field of solvent and that it is most easily to be polarized. Shown in Figure 4 is alteration of PCF due to temperature change, $\Delta_{\text{Tg}}(T) = g(T) - g(273.15 \text{ K})$. The oxygen site of hydronium ion has the least negative charge among the three species, and $\Delta_{\text{Tg}}(T)$ is rather loose and broad. But, changes in the others are extremely sharp and large. Especially, a negative deviation around 2.0 Å corresponds to change in height of the first peak in PCF, being indicative of a drastic change in hydrogen bonds as temperature increases. It should be noted that Δ_{Tg} in hydroxide ion is about 10 times greater than that in water. The positive deviation around 1.5 Å is a consequence of the increased probability of repulsive configurations with increasing temperature and can be compared with the results reported for the temperature derivatives of the ion-water PCF.²³

3.3. Temperature Dependence of Free Energy and $\text{p}K_w$. Free energy components in aqueous solution at selected temperatures are listed in Table 2. The three upper groups in the table include energy components of each species. The kinetic term G_{kin} contributed from the kinetic energies decreases with increasing temperature, which can be understood by the elementary statistical mechanics. The temperature dependence

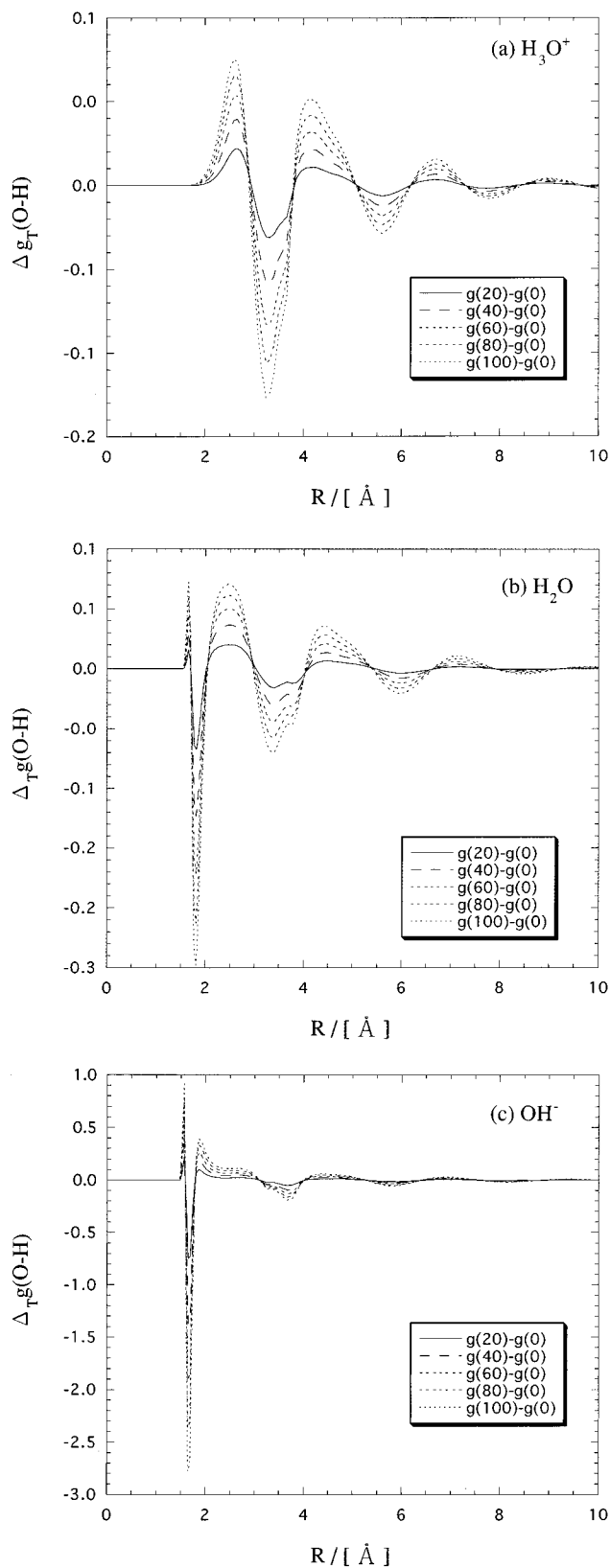


Figure 4. Temperature dependence of PCF: (a) hydronium ion; (b) water; (c) hydroxide ion.

of δE_{elec} can be explained in terms of the polarization of solute (i.e., effective charge) and solvation structure discussed in the previous section. As has been discussed there, the electronic structure on each species is relaxed toward that in the gas phase upon rising temperature. Thus, δE_{elec} decreases as temperature increases. It is noteworthy that δE_{elec} of hydroxide ion is

TABLE 2: Free Energy Component at Selected Temperature^a

	273.15 K	293.15 K	373.15 K
H₂O			
δE_{elec}	2.38	2.27	1.87
$\delta\mu$	-5.17	-4.58	-2.94
δG_{kin}	7.45	6.89	4.52
δG	4.67	4.58	3.45
H₃O⁺			
δE_{elec}	3.74	3.59	3.11
$\delta\mu$	-73.49	-72.33	-68.38
δG_{kin}	15.38	14.77	12.23
δG	-54.37	-53.97	-53.04
OH⁻			
δE_{elec}	9.43	8.93	7.15
$\delta\mu$	-140.02	-137.95	-130.17
δG_{kin}	0.20	-0.29	-2.33
δG	-130.39	-129.31	-125.35
Energy Difference			
$\Delta E_{\text{elec}}^{\text{vac}}$	229.54	229.54	229.54
$\Delta\delta E_{\text{elec}}$	8.41	7.98	6.53
$\Delta\delta\mu$	-203.17	-201.13	-192.67
$\Delta\delta G_{\text{kin}}$	0.67	0.71	0.87
ΔG^{aq}	35.45	37.10	44.27

^a All the energies are given in kcal/mol.

estimated 2 or 3 times larger than those of any other species, being consistent with the finding in the previous section, that the anion is more polarizable than the other species. Our results for the excess chemical potential, $\delta\mu$, or the hydration free energy are in good agreement with those reported by other authors based on the dielectric continuum models. For the hydration energy of hydronium ion, for instance, Emsley et al.⁵ and Chipot et al.³ reported -74.6 to -89.2 kcal/mol and -78.8 kcal/mol, respectively, which are very close to our estimation at the room temperature (293.15 K), -72.33 kcal/mol. The hydration free energy of each species increases, or changes toward more positive side, with increasing temperature, which reflects reduced electrostatic interactions including the hydrogen bonding due to increased thermal motions. The change is much greater for OH⁻ (~ 9.9 kcal/mol) than for H₂O (~ 2.2 kcal/mol) and H₃O⁺ (~ 5.1 kcal/mol) in this range of temperatures. The behavior can be again ascribed to the characteristics of the anion which is more polarizable than the other species. The total free energy of each species is determined by a subtle balance among these components, and only H₂O shows a decrease with rising temperature.

Changes in the free energy components associated with the autoionization reaction (eq 1), are listed in the bottom group of Table 2. The temperature dependence of the energy difference is also plotted in Figure 5. Since $\Delta\delta\mu$'s and $\Delta E_{\text{elec}}^{\text{vac}}$ are greater in magnitude by a few orders compared to the other components, and since they largely compensate each other, we plot the sum of those contributions. It is important to note that the sum $\Delta E_{\text{elec}}^{\text{vac}} + \Delta\delta\mu$ shows a rather large positive temperature dependence. Compared to these contributions, $\Delta\delta G_{\text{kin}}$ is almost negligible in the present level of estimations both in magnitudes and in temperature dependence. $\Delta\delta E_{\text{elec}}$ shows a small and negative dependence on temperature, to which the main contribution comes from the hydroxide ion.

Finally, we show a resultant $\Delta_{\text{TP}}K_{\text{w}}$ and their components in Figure 6. $\Delta_{\text{TP}}K_{\text{w}}$ is decomposed into the following four terms:

$$\Delta_{\text{TP}}K_{\text{w}}(T) = \Delta_{\text{TP}}K_{\text{w,elec}}^{\text{vac}} + \Delta_{\text{TP}}K_{\text{w, reorg}}(T) + \Delta_{\text{TP}}K_{\text{w,}\delta\mu}(T) + \Delta_{\text{TP}}K_{\text{w,kin}}(T) \quad (11)$$

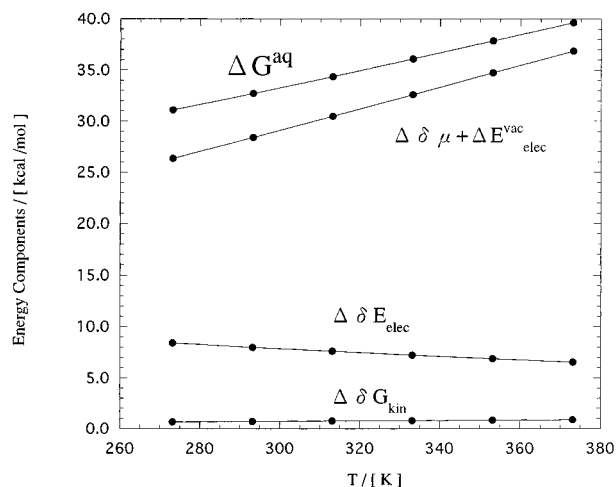


Figure 5. Temperature dependence of free energy and its components.

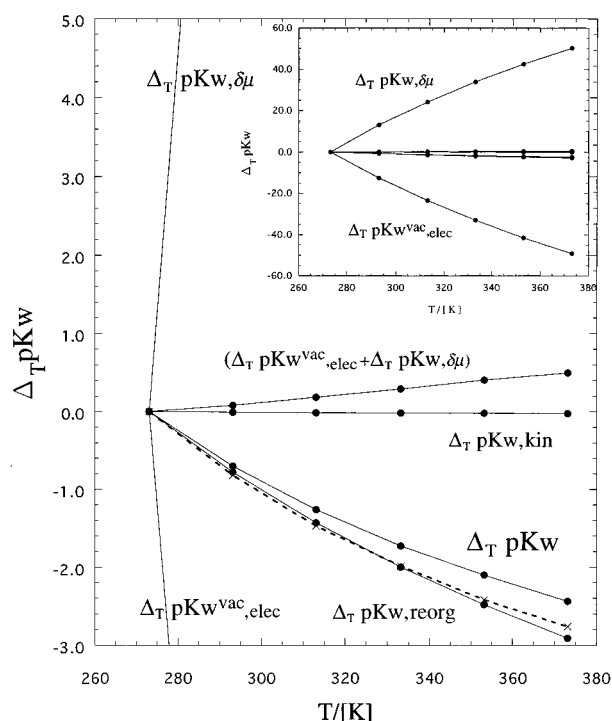


Figure 6. Temperature dependence of pK_w of water. Dashed line indicates the experimentally observed value, while all other solid lines are computed by the RISM-SCF/MCSCF procedure.

where $\Delta_T pK_{w,\text{elec}}^{\text{vac}}$, $\Delta_T pK_{w,\text{reorg}}$, $\Delta_T pK_{w,\delta\mu}$, and $\Delta_T pK_{w,\text{kin}}$ are related respectively to the corresponding free energy changes, $\Delta E_{\text{elec}}^{\text{vac}}$, $\Delta\delta E_{\text{elec}}$, $\Delta\delta\mu$, and $\Delta\delta E_{\text{kin}}$ by eq 9. To facilitate the inspection, a sum of $\Delta_T pK_{w,\delta\mu}$ and $\Delta_T pK_{w,\text{elec}}^{\text{vac}}$ is also plotted in the figure. Those contributions are very large, but they compensate each other, and the sum shows slight and positive dependence on temperature. It is important to note that the components in $\Delta_T pK_w$ show different temperature dependence from corresponding terms in $\Delta G^{\text{aq}}(T)$ due to “ T ” which appears in the denominator in eq 10. It is readily seen from the figure that the temperature dependence of pK_w is determined by an interplay of several contributions with different physical origins. It is also clear that the temperature dependence is dominated by $\Delta_T pK_{w,\text{reorg}}$ after the largest contributions compensated each other. As a consequence, the theoretical results for the temperature dependence of the ionic product show good agreement with experiments.

To summarize, the so-called solvation free energies, or $\delta\mu$, contribute to a positive temperature dependence on $\Delta_T pK_w$, while the energies associated with reorganization of electronic structure give rise to the opposite temperature dependence. In other words, the solvation free energies contribute to make a water molecule less dissociative with increasing temperature, which is in accord with the intuitive consideration in terms of the reduced hydrogen bonding. On the other hand, the electronic reorganization energy contributes to facilitate the dissociation as temperature increases. The latter dominates the temperature dependence of the ionic product. The temperature dependence is in turn largely determined by characteristics of the electronic structure of OH^- , because the temperature dependence of the electronic reorganization energy is dominated by that species.

Improvements of the theoretical calculations, especially in descriptions of electronic structures, can be expected for ΔpK_w . However, as long as the temperature dependence is concerned, the qualitative feature of our results seems to be insensitive to our preliminary calculations based on the second-order Møller–Plesset perturbation.

Acknowledgment. The present study is supported by Grants-in-Aid for Scientific Research from the Japanese Ministry of Education, Science, Sports, and Culture.

References and Notes

- (1) Pearson, R. G. *J. Am. Chem. Soc.* **1986**, *108*, 6109.
- (2) Tuckerman, M.; Laasonen, K.; Sprik, M.; Parrinello, M. *J. Phys. Chem.* **1995**, *99*, 5749.
- (3) Chipot, C.; Gorb, L. G.; Rivail, J.-L. *J. Phys. Chem.* **1994**, *98*, 1601.
- (4) Tortonada, F. R.; Pascual-Ahuir, J.-L.; Silla, E.; Tuñón, I. *J. Phys. Chem.* **1993**, *97*, 11087.
- (5) Emsley, J.; Lucas, J.; Overill, R. E. *Chem. Phys. Lett.* **1981**, *84*, 593.
- (6) Gao, J. *Acc. Chem. Res.* **1996**, *29*, 298.
- (7) Tanaka, Y.; Shiratori, Y.; Nakagawa, S. *Chem. Phys. Lett.* **1990**, *169*, 513.
- (8) Ten-no, S.; Hirata, F.; Kato, S. *Chem. Phys. Lett.* **1993**, *214*, 391.
- (9) Ten-no, S.; Hirata, F.; Kato, S. *J. Chem. Phys.* **1994**, *100*, 7443.
- (10) (a) Sato, H.; Hirata, F.; Kato, S. *J. Chem. Phys.* **1996**, *105*, 1546.
- (11) (a) Kawata, M.; Ten-no, S.; Kato, S.; Hirata, F. *Chem. Phys.* **1996**, *203*, 53. (b) Kawata, M.; Ten-no, S.; Kato, S.; Hirata, F. *J. Phys. Chem.* **1996**, *100*, 1111.
- (12) Chandler, D.; Andersen, H. C. *J. Chem. Phys.* **1972**, *57*, 1930.
- (13) Hirata, F.; Rossky, P. J. *Chem. Phys. Lett.* **1981**, *84*, 329.
- (14) Dobos, D. *Electrochemical Data; a Handbook for Electrochemists in Industry and Universities*; Elsevier Scientific Publishing: Amsterdam, 1975.
- (15) Poirier, R.; Kari, R.; Csizmadia, I. G. *Handbook of Gaussian Basis Set*; Elsevier: New York, 1985; Physical Science Data 24.
- (16) Berendsen, H. J. C.; Postma, J. P. M.; van Gunsteren, E. F. J.; Hermans, J. *Intermolecular Forces*; Pullman, B., Ed.; Reidel: Dordrecht, 1981.
- (17) *CRC Handbook of Chemistry and Physics*, 68th ed.; CRC Press: Boca Raton, FL, 1987.
- (18) Hill, T. L. *Statistical Mechanics*; McGraw-Hill: New York, 1956.
- (19) (a) Chandler, D.; Pratt, L. R. *J. Chem. Phys.* **1976**, *65*, 2925. (b) Pratt, L. R.; Chandler, D. *J. Chem. Phys.* **1977**, *66*, 147. (c) Pratt, L. R.; Chandler, D. *J. Chem. Phys.* **1977**, *67*, 3683.
- (20) Munakata, T.; Yoshida, S.; Hirata, F. *Phys. Rev. E* **1996**, *54*, 3687.
- (21) Maw, S.; Sato, H.; Ten-no, S.; Hirata, F. *Chem. Phys. Lett.*, in press.
- (22) Ichikawa, K.; Kameda, Y.; Yamaguchi, T.; Wakita, H.; Misawa, M. *Mol. Phys.* **1991**, *73*, 79.
- (23) Corongiu, G.; Clementi, E. *J. Chem. Phys.* **1992**, *97*, 2030.
- (24) Chong, S.-H.; Hirata, F. *J. Phys. Chem. B* **1997**, *101*, 3209.
- (25) Thiessen, W. E.; Narten, A. H. *J. Chem. Phys.* **1982**, *77*, 2656.
- (26) Walford, G.; Clarke, J. H.; Dore, J. C. *Mol. Phys.* **1977**, *33*, 25.
- (27) Moriarty, N. W.; Karlström, G. *J. Chem. Phys.* **1997**, *106*, 6470.
- (28) Chesnut, D. B.; Rusiloski, B. E. *J. Mol. Struct. (THEOCHEM)* **1994**, *314*, 19.